PHOTONICS Research

Strong mechanical squeezing in an optomechanical system based on Lyapunov control

Biao Xiong,[1] Xun Li,[1] Shi-Lei Chao,[1] Zhen Yang,[1] Wen-Zhao Zhang,[2] Weiping Zhang,[3,4] and Ling Zhou[1,*]

[1]School of Physics, Dalian University of Technology, Dalian 116024, China
[2]Department of Physics, Ningbo University, Ningbo 315211, China
[3]Department of Physics and Astronomy, Shanghai Jiao Tong University, Shanghai 200240, China
[4]Collaborative Innovation Center of Extreme Optics, Shanxi University, Taiyuan 030006, China
*Corresponding author: zhlhxn@dlut.edu.cn

Received 24 July 2019; revised 28 October 2019; accepted 26 November 2019; posted 27 November 2019 (Doc. ID 373535); published 24 January 2020

We propose a scheme to generate strong squeezing of a mechanical oscillator in an optomechanical system through Lyapunov control. Frequency modulation of the mechanical oscillator is designed via Lyapunov control. We show that the momentum variance of the mechanical oscillator decreases with time evolution in a weak coupling case. As a result, strong mechanical squeezing is realized quickly (beyond 3 dB). In addition, the proposal is immune to cavity decay. Moreover, we show that the obtained squeezing can be detected via an ancillary cavity mode with homodyne detection.

https://doi.org/10.1364/PRJ.8.000151

1. INTRODUCTION

Quantum fluctuation is the essential characteristic of quantum mechanics. Reducing quantum fluctuation below the standard fluctuation of zero-point level, called quantum squeezing, is always worth investigation [1], because quantum squeezing on the one hand plays an important role in fundamental physics, such as exploring the quantum-classical boundary [2–4], and on the other hand has an important value in practical applications, which include improving ultrasensitive detection [5–8] and enhancing coupling [9–11]. Squeezing of the mechanical mode is of special interest. The demonstration of mechanical squeezing was first reported in Ref. [12], using a spring constant tuned silicon microcantilever. With the development of quantum optics and the needs of precise quantum measurement, schemes realizing mechanical squeezing based on various systems, for instance the NV-center system [13] and trapped-ion system [14], have subsequently been proposed.

The cavity optomechanical system, due to the interaction between the cavity field and mechanical motion, provides us with a promising platform for high-precision measurements [15–18]. Therefore, the mechanical squeezing is necessary in the cavity optomechanical system in order to reduce additional noise [19–21]. The basic mechanism for generating mechanical squeezing is to introduce a mechanical parametric amplification in the cavity optomechanical system [22–25]. Using the mechanical parametric amplification, the squeezing of the mechanical oscillator has been achieved both theoretically and experimentally [26,27]. However, the squeezing can be restricted by the so called 3 dB limit due to the instability caused by the parametric amplification process [28–30]. To surpass the 3 dB limit of mechanical squeezing, schemes including injecting a squeezed light into the cavity [31,32], kicking the mechanical mode by the bang-bang control technique [33], jointing the effect between Duffing nonlinearity and parametric pump driving [34], and applying continuous weak measurement and feedback to the system [35] have been proposed. Recently, strong squeezing of the mechanical oscillator is demonstrated via the coherent feedback process, which can be performed by driving the cavity with two-tone driven field [36–40] or introducing a sine modulation of the free term to the mechanical oscillator in the optomechanical system [41].

On the other hand, quantum control is a powerful tool in modern quantum technologies [42–44]. In the Lyapunov control method, an index function (i.e., Lyapunov function) can monotonically increase or decrease to the target by designing the control field. Until now, Lyapunov control has been successfully used for processing diverse quantum tasks, such as realizing quantum synchronization [45], speeding up adiabatic passage [46], preparing quantum states [47], and designing quantum optical diode [48]. With the advances of microscale and nanoscale fabrication, it is becoming possible to engineer and to control the mechanical oscillator in the cavity optomechanical system. Recently, the mechanical oscillator with tunable frequency has been reported experimentally [49]. With the engineered mechanical oscillator, the quantum process, such as cooling [50] and squeezing [41], can be enhanced.

Although Lyapunov control and the optomechanical system have both been extensively studied separately, there are few studies which employ Lyapunov control to manipulate the optomechanical system. In this paper, by introducing a modulation of the frequency to the mechanical oscillator, a scheme to generate strong mechanical squeezing in an optomechanical system is proposed. Unlike modulating the frequency of the mechanical resonator periodically as in previous research [41,50,51], in our scheme, the frequency variations are designed based on Lyapunov control theory. By designing special time-varying mechanical frequency, the momentum variance of the mechanical mode can be decreased with time evolution, which results in the strong mechanical squeezing (larger than 10 dB in our parameter region). Moreover, the squeezing is immune to cavity decay in the weak coupling regime.

Our proposal generating mechanical squeezing based on Lyapunov control has three distinct merits. First, we can quickly obtain the strong squeezing, since the momentum variance of the mechanical oscillator decreases monotonically without oscillation. Second, our scheme generates squeezing without using assistant squeezing source. Therefore, the complexity of the experiment may be reduced. Third, as there is no parametric amplification term in our system, the instability caused by parametric amplification is avoided, thus leading to the squeezing beyond 3 dB possible.

The rest of this paper is organized as follows. We first briefly introduce the method of quantum Lyapunov control in Section 2. Then we present the model and its solution in Section 3. In Section 4, we discuss the generation of mechanical squeezing by employing the Lyapunov control. In Section 5, we give the proposal for detecting the obtained mechanical squeezing. The discussions and conclusions are summarized in Section 6.

2. METHOD OF QUANTUM LYAPUNOV CONTROL

We first briefly review quantum Lyapunov control method. For a controlled system, the total Hamiltonian can be generally expressed as

$$H = H_{\rm res} + \sum_n f_n(t) H_n, \tag{1}$$

where H_n is the control Hamiltonian, and $f_n(t)$ is the time-varying control field with $n = 1, 2, \ldots$. $H_{\rm res}$ is the rest Hamiltonian except the control Hamiltonian. The index function, which is also known as the Lyapunov control function, is selected according to the purpose. Here, we consider the mean value of operator O as the index function, i.e., $V(t) = \langle O \rangle = {\rm Tr}(\rho O)$. In the interaction picture, we have

$$\dot{O} = -i\left[O, H_{\rm res} + \sum_n f_n(t) H_n\right]. \tag{2}$$

Therefore, the derivative of control function $V(t)$ satisfies

$$\dot{V}(t) = {\rm Tr}(\rho \dot{O}) = \sum_n f_n(t) \langle -i[O, H_n] \rangle, \tag{3}$$

where for simplicity, $[O, H_{\rm res}] = 0$ is assumed to obtain Eq. (3). Actually, even if $[O, H_{\rm res}] \neq 0$, we can design one of the terms in the control field to cancel $\langle -i[O, H_{\rm res}] \rangle$, hence we can always obtain the above equation. Supposing we want to reduce $\langle O \rangle$, we can design the control field as $f_n(t) = -c\langle -i[O, H_n] \rangle^*$ $(c > 0)$. The derivative of $V(t)$ then becomes

$$\dot{V}(t) = \langle \dot{O} \rangle = -c \sum_n |\langle -i[O, H_n] \rangle|^2. \tag{4}$$

We see that $\dot{V}(t) \leq 0$ is always satisfied, which means $\langle O \rangle$ will decrease monotonically during evolution. Therefore, the purpose of control has been realized by the selection of the control field $f_n(t) = -c\langle -i[O, H_n] \rangle^*$. It should be noted that although $f_n(t)$ seems to depend on the evolution of $\langle -i[O, H_n] \rangle^*$, we do not need to measure the value of $\langle -i[O, H_n] \rangle^*$. The control field is actually obtained by the simulation, which is measurement-independent. In the experiment, one can pulse the simulated control field to the system, and the system will evolve toward the goal of design. In the following, we will decrease the momentum variance of the mechanical oscillator based on the Lyapunov control method, so as to obtain strong squeezing of the mechanical oscillator.

3. MODEL AND SOLUTION

The system under consideration is a cavity optomechanical system, where a frequency-tunable mechanical oscillator couples to a single-mode cavity with the coupling strength g_0, as schematically shown in Fig. 1. To tune the frequency of the mechanical resonator, one can apply a gate voltage V_g between the mechanical oscillator and the underlying electrode experimentally [52–54], or couple the mechanical oscillator with a low-Q driven assisted mode (see Appendix A for details). The Hamiltonian of the system then reads

$$H = \hbar\omega_c a^\dagger a + \frac{p_x^2}{2m} + \frac{1}{2} m\omega_r^2(t) x^2 - \hbar g a^\dagger a x + i\hbar E(e^{-i\omega_d t} a^\dagger - e^{i\omega_d t} a), \tag{5}$$

where a ($a^\dagger$) is the annihilation (creation) operator of the cavity mode with the resonant frequency ω_c, and x and p_x are the position and momentum operators of the mechanical resonator. Here $\omega_r(t)$ is the controllable frequency of the mechanical mode tuned from the static frequency ω_m and can be modulated by V_g. The last term in Eq. (5) describes the external classical driving to the cavity with the driven amplitude E and frequency ω_d. By introducing the dimensionless position and momentum operators of the mechanical resonator (q, p) through

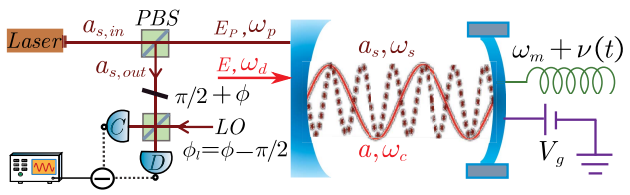

Fig. 1. Schematic of the considered system, where the mechanical frequency is modulated through the tuning electrode. The left setups are used to detect the obtained mechanical squeezing.

$$q=\sqrt{\frac{m\omega_m}{\hbar}}x,\qquad p=\frac{p_x}{\sqrt{\hbar m\omega_m}},\tag{6}$$

the Hamiltonian of Eq. (5) can be rewritten as

$$H=\hbar\omega_c a^\dagger a+\frac{\hbar\omega_m}{2}p^2+\frac{\hbar\omega_r^2(t)}{2\omega_m}q^2-\hbar g_0 a^\dagger a q+i\hbar E(e^{-i\omega_d t}a^\dagger-e^{i\omega_d t}a).\tag{7}$$

In the interaction picture with $H_0=\hbar\omega_d a^\dagger a$, and taking the dissipation and noise into consideration, we can write the quantum Langevin equations of the system as

$$\begin{aligned}\dot q&=\omega_m p,\\ \dot p&=-\frac{\omega_r^2(t)}{\omega_m}q-\gamma p+g_0 a^\dagger a+\xi,\\ \dot a&=-(\kappa+i\Delta_c)a+ig_0 aq+E+\sqrt{2\kappa}a_{in},\end{aligned}\tag{8}$$

where $\Delta_c=\omega_c-\omega_d$ is the detuning between the cavity mode and driven field, and κ and γ represent the damping rates of the optical mode and mechanical mode, respectively. The noise operators $a_{\rm in}$ and ξ satisfy the following correlation functions:

$$\begin{aligned}\langle a_{\rm in}(t)a_{\rm in}^\dagger(t')\rangle&=(\bar n_c^T+1)\delta(t-t'),\\ \langle\xi(t)\xi(t')+\xi(t')\xi(t)\rangle/2&=\gamma(2\bar n_m^T+1)\delta(t-t'),\end{aligned}\tag{9}$$

under Markovian approximation, where $\bar n_c^T$ and $\bar n_m^T$ are the equilibrium mean thermal photon numbers of the cavity mode and mechanical oscillator, respectively. Generally, $\bar n_c^T\approx 0$ due to the high optical frequency.

By performing the standard linearization process, we write the operators as their mean values plus small quantum fluctuations, i.e., $a=\alpha+\delta a$, $q=q_c+\delta q$, $p=p_c+\delta p$, where α, q_c, and p_c are complex numbers determined by

$$\begin{aligned}\dot q_c&=\omega_m p_c,\\ \dot p_c&=-\frac{\omega_r^2(t)}{\omega_m}q_c-\gamma p_c+g_0|\alpha|^2,\\ \dot\alpha&=-(\kappa+i\Delta_c')\alpha+E,\end{aligned}\tag{10}$$

with $\Delta_c'=\Delta_c-g_0 q_c$. Correspondingly, the fluctuation parts satisfy

$$\begin{aligned}\dot{\delta q}&=\omega_m\delta p,\\ \dot{\delta p}&=-\frac{\omega_r^2(t)}{\omega_m}\delta q-\gamma\delta p+G(\delta a^\dagger+\delta a)+\xi,\\ \dot{\delta a}&=-(\kappa+i\Delta_c')\delta a+iG\delta q+\sqrt{2\kappa}a_{\rm in},\end{aligned}\tag{11}$$

where $G=g_0\alpha$ is the effective coupling rate. It should be pointed out that G can achieve any desirable value in principle by modulating the corresponding driving $E(t)$ [55,56]. By introducing the quadrature operators $\delta X=(\delta a+\delta a^\dagger)/\sqrt{2}$, $\delta Y=(\delta a-\delta a^\dagger)/\sqrt{2}i$ and the corresponding noise operators $X_{\rm in}=(a_{\rm in}+a_{\rm in}^\dagger)/\sqrt{2}$, $Y_{\rm in}=(a_{\rm in}-a_{\rm in}^\dagger)/\sqrt{2}i$, the linearized Langevin equations for the fluctuation operators can be concisely expressed as

$$\dot u(t)=A(t)u(t)+N(t),\tag{12}$$

where $u(t)=(\delta X(t),\delta Y(t),\delta q(t),\delta p(t))^T$, $N(t)=(\sqrt{2\kappa}X_{\rm in}(t),\ \sqrt{2\kappa}Y_{\rm in}(t),\ 0,\ \xi(t))^T$, and $A(t)$ is

$$A(t)=\begin{pmatrix}-\kappa & \Delta_c' & 0 & 0\\ -\Delta_c' & -\kappa & \sqrt{2}G & 0\\ 0 & 0 & 0 & \omega_m\\ \sqrt{2}G & 0 & -\omega_r^2(t)/\omega_m & -\gamma\end{pmatrix}.\tag{13}$$

The formal solution of Eq. (12) can then be given as

$$u(t)=L(t)u(0)+L(t)\int_0^t d\tau' L^{-1}(\tau')N(\tau'),\tag{14}$$

where $L(t)=\mathcal{T}\exp[\int_0^t d\tau A(\tau)]L(0)$ with $\mathcal{T}$ the time order operator.

To calculate the quantum fluctuation of the mechanical mode, we introduce the covariance matrix $R(t)$ defined as

$$R_{ij}(t)=[\langle u_i(t)u_j(t)+u_j(t)u_i(t)\rangle]/2.\tag{15}$$

By using Eqs. (14) and (15), we can obtain

$$R=L(t)R(0)L^T(t)+L(t)M(t)L^T(t),\tag{16}$$

where

$$\begin{aligned}M(t)&=\frac{1}{2}[W(t)+W^T(t)],\\ W(t)&=\int_0^t d\tau\int_0^t d\tau' L^{-1}(\tau')C(\tau,\tau')[L^{-1}(\tau)]^T.\end{aligned}\tag{17}$$

Here $C(\tau,\tau')$ is the noise operator correlation matrix with its matrix element $C_{ij}(\tau,\tau')=\langle N_i(\tau)N_j(\tau')\rangle$. Obviously

$$\langle N_{ij}(\tau)N_{ij}(\tau')+N_{ij}^T(\tau)N_{ij}^T(\tau')\rangle/2=D_{ij}\delta(\tau-\tau').\tag{18}$$

Here, D_{ij} is the matrix element of the diagonal matrix $D=\mathrm{Diag}[\kappa,\kappa,0,\gamma(2\bar n_m^T+1)]$. Substituting Eq. (18) into Eq. (17), we obtain

$$M(t)=\int_0^t d\tau L^{-1}(\tau)D(\tau)[L^{-1}(\tau)]^T.\tag{19}$$

By substituting Eq. (19) into Eq. (16), the derivative of the covariance matrix is given by

$$\dot R(t)=A(t)R(t)+R(t)A^T(t)+D.\tag{20}$$

For a mechanical oscillator, the rotating quadrature operator is $X(\theta,t)=\cos\theta\cdot\delta q+\sin\theta\cdot\delta p$. Correspondingly, the variance of the mechanical quadrature operator $\Delta X^2=\langle X^2(\theta,t)\rangle-\langle X(\theta,t)\rangle^2$ is given by

$$\begin{aligned}\Delta X^2&=\cos^2\theta\langle\delta q^2\rangle+\sin^2\theta\langle\delta p^2\rangle+\frac{1}{2}\sin 2\theta(\langle\delta q\delta p\rangle+\langle\delta p\delta q\rangle)\\ &=\cos^2\theta R_{33}+\sin^2\theta R_{44}+\frac{1}{2}\sin 2\theta(R_{34}+R_{43}).\end{aligned}\tag{21}$$

Therefore the variance of the quadrature operator $X(\theta,t)$ for the mechanical mode can be obtained by solving Eq. (20) with the initial condition $R(0)=\mathrm{Diag}[1/2,1/2,1/2,1/2]$. Here the initial fluctuation 1/2 means the cavity and mechanical fields are both in vacuum states, which can be realized by respectively precooling the cavity mode and mechanical resonator to their ground states.

4. GENERATION OF MECHANICAL SQUEEZING WITH LYAPUNOV CONTROL

Now we employ the Lyapunov control method introduced in Section 2 to generate the mechanical quadrature squeezing. The index ΔX^2 is selected as the Lyapunov function $V(t)$, i.e., $V(t) = \Delta X^2$. Obviously, $V(t) > 0$. And the time derivative of $V(t)$ by using Eq. (21) is calculated as

$$\dot{V}(t) = \cos^2\theta \dot{R}_{33} + \sin^2\theta \dot{R}_{44} + \frac{1}{2}\sin 2\theta(\dot{R}_{34} + \dot{R}_{43}), \tag{22}$$

where

$$\begin{aligned}
\dot{R}_{33} &= \omega_m(R_{34} + R_{43}),\\
\dot{R}_{44} &= -2\gamma R_{44} - \frac{\omega_r(t)^2}{\omega_m}(R_{34} + R_{43})\\
&\quad + \sqrt{2}G(R_{14} + R_{41}) + \gamma(2\tilde{n}_m^T + 1),\\
\dot{R}_{34} &= \omega_m R_{44} - \frac{\omega_r(t)^2}{\omega_m}R_{33} - \gamma R_{34} + \sqrt{2}GR_{31},\\
\dot{R}_{43} &= \omega_m R_{44} - \frac{\omega_r(t)^2}{\omega_m}R_{33} - \gamma R_{43} + \sqrt{2}GR_{13}.
\end{aligned} \tag{23}$$

In our model, $\omega_r(t)$ is adjustable, and therefore we can select $\omega_r(t)$ as a control field. However, only the static frequency ω_m appears in the first equation of Eq. (23), thus the first term of Eq. (22) is not controllable. Therefore, we can set $\theta = \pi/2$ to cancel the first term of Eq. (22) for simplicity. In this case, the Lyapunov function $V(t) = \Delta p^2$ is the variance of momentum operator. Then the time derivative of $V(t)$ becomes

$$\begin{aligned}
\dot{V}(t) &= -2\gamma R_{44} - \frac{\omega_r^2(t)}{\omega_m}(R_{34} + R_{43}) + \sqrt{2}G(R_{14} + R_{41})\\
&\quad + \gamma(2\tilde{n}_m^T + 1).
\end{aligned} \tag{24}$$

In the right-hand side of the above equation, the first term $-\gamma R_{44} < 0$ is always satisfied. And if we choose the control field $\omega_r^2(t) = c\omega_m(R_{34} + R_{43})$ with $c > 0$, the second term $-\frac{\omega_r^2(t)}{\omega_m}(R_{34} + R_{43}) = -c|R_{34} + R_{43}|^2 \le 0$. In principle, we can choose $G = -c_2(R_{14} + R_{41})$ with $c_2 > 0$ to guarantee the third term $\sqrt{2}G(R_{14} + R_{41}) \le 0$. However this setting is not necessary, because the correlation between the cavity field and mechanical oscillator R_{14} and R_{41} is small. At the weak coupling case, the effect of the third term can be neglected. For high quality factor mechanical oscillator and low bath temperature, the last term $\gamma(2\tilde{n}_m^T + 1)$ contributes small to the equation of derivative of V. For the convenience of analysis, we ignore the influence of the last two terms. And in the numerical simulations, we do not use this approximation. If ignoring the last two terms,

$$\dot{V}(t) \approx -2\gamma R_{44} - c|R_{34} + R_{43}|^2, \tag{25}$$

with

$$\omega_r^2(t) = c\omega_m(R_{34} + R_{43}). \tag{26}$$

It is obvious that $\dot{V}(t)$ is always less than or equal to zero, which means the index function $V(t) = \Delta p^2$ will decrease monotonically during evolution, and may approach 0 with $\omega_r^2(t) = c\omega_m(R_{34} + R_{43})$. Therefore, the momentum variance of mechanical oscillator Δp^2 can be reduced to below the zero-point level, as a result the squeezed mechanical oscillator is obtained. We should note that although $\omega_r^2(t) = c\omega_m(R_{34} + R_{43})$ is dependent of $R_{34} + R_{43}$, the experimental detection of $R_{34} + R_{43}$ is not necessary, and the control field $\omega_r^2(t)$ is obtained by simulation. This is an open-loop control scheme, which uses the closed-loop idea to solve the problem of open-loop control.

To examine the above analysis, we need to simulate the dynamics of the system. In Fig. 2(a), the momentum variance of mechanical oscillator Δp^2 depending on time at $G = 0.1\omega_m$ is plotted, in which case the time-varying frequency of the mechanical oscillator is shown in Fig. 2(c). It is obvious that Δp^2 decreases monotonically with time evolution as shown by the solid blue line, which agrees with the above discussions. Without control, we see that Δp^2 oscillates near the zero-point level 0.5. However, with the Lyapunov control, Δp^2 will be lower than 0.1, and thus we realize strong squeezing of the mechanical oscillator. The evolution of momentum variance Δp^2 at $G = 0.5\omega_m$ is shown in Fig. 2(b). Correspondingly, in Fig. 2(d), we give the time-dependent mechanical frequency for the control case. With this higher coupling strength, we see that Δp^2 is still oscillating around 0.5 without control. Although Δp^2 does not always decrease with respect to time t with the Lyapunov control, the stable Δp^2 is about 0.355, which means we can still realize squeezing at $G = 0.5\omega_m$.

In Figs. 3(a) and 3(b), we further study the control effect of the control field described by Eq. (26) under different G and Δ_c', while Figs. 3(c) and 3(d) are the control fields. It is seen that the larger G is, the less monotonic Δp^2 is. This is resonant because Eq. (25) is obtained in the approximation by neglecting the effect of $\sqrt{2}G(R_{14} + R_{41})$ as described in Eq. (24), and this approximation is only valid for the weak coupling case. For ultrastrong coupling G, Δp^2 will oscillate with time evolution and the squeezing will disappear; therefore, the above Lyapunov control scheme is valid for the weak coupling case. In principle, the squeezing is best with $G = 0$, while squeezing in the cavity optomechanical system is of significance, so we discuss the

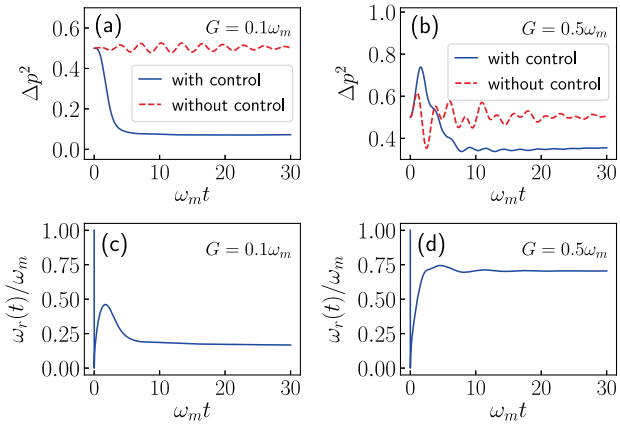

Fig. 2. (a) and (b) show time evolution of Δp^2 with the time-varying frequency $\omega_r(t)$ at the control case presented in (c) and (d), respectively, where $\Delta_c' = \omega_m$, $\kappa = 0.1\omega_m$, $\gamma = 10^{-6}\omega_m$, $\tilde{n}_m^T = 0$, and $c = 0.2$.

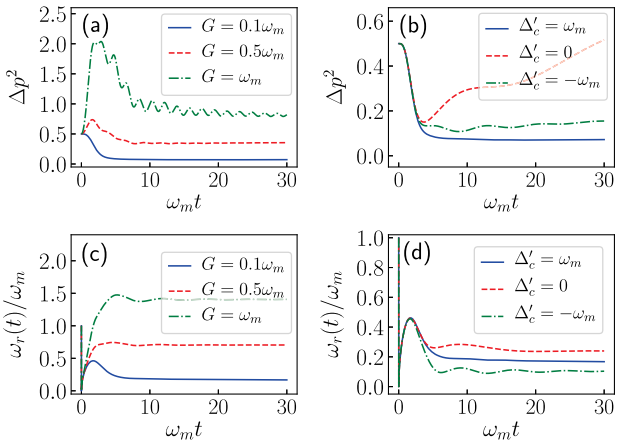

Fig. 3. Time evolution of Δp^2 at different G and Δ_c' in (a) and (b), respectively, where (c) and (d) are the corresponding time-varying control fields. The other parameters are the same as in Fig. 2.

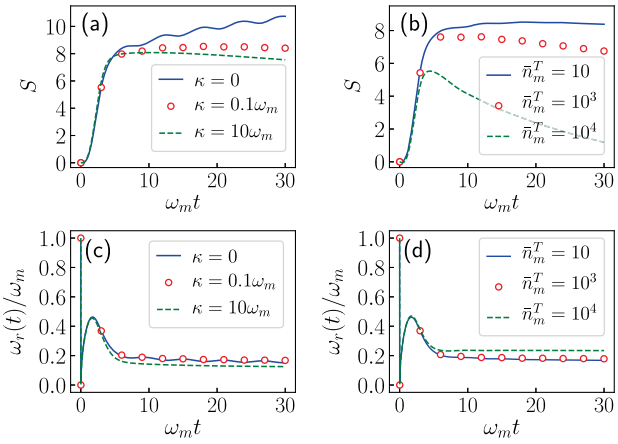

Fig. 5. Plot of squeezing level with different cavity decay κ in (a) and thermal phonon number $\bar{n}_m^T$ in (b). (c) and (d) are the corresponding control fields. The other parameters are the same as in Fig. 2(a).

squeezing with $G \neq 0$. In Fig. 3(b), it is obvious that the above Lyapunov control scheme works well for the sideband regime, especially for the red sideband case. Generally speaking, the red sideband condition $\Delta_c' = \omega_m$ is used for the ultrasensitive detection; therefore, the squeezing generated by our scheme may be useful for enhancing ultrasensitive detection.

In order to clearly see the squeezing intuitively, we present the Wigner function of mechanical oscillator W_m in Fig. 4. It is obvious that W_m has the same distribution on q and p at $\omega_m t = 0$; hence, there exists no squeezing at the initial time. With the time evolution, when $\omega_m t = 30$, the mechanical quadrature p is obviously squeezed, and the maximum squeezed direction is along the position p.

To further study the robustness of our scheme, we now simulate the squeezing level S as a function of time t with different cavity decay κ and thermal phonon number $\bar{n}_m^T$, where the squeezing level S in the decibel unit is defined by

$$S = -10\log_{10}(\Delta p^2/\Delta p_{zp}^2). \tag{27}$$

Here $\Delta p_{zp}^2 = 0.5$ is the standard fluctuation in the zero-point level.

Figure 5(a) shows that the proposed scheme is affected little by the cavity decay κ. When the system changes from the resolved sideband regime to the unresolved sideband regime, the squeezing level S decreases a little. This is reasonable since the cavity field has little effect on the proposal in the weak coupling regime as discussed above. Hence our scheme is robust to cavity decay. Moreover, the squeezing level can surpass 3 dB limit at a fast time, which suggests that the strong squeezing of the mechanical oscillator can be attained quickly even at large cavity decay. From Fig. 5(b), we see that the squeezing level S decreases a lot when the thermal phonon number $\bar{n}_m^T$ increases from 10 to 10^4. This can be understood by Eq. (24). With large $\bar{n}_m^T$, the term $\gamma(2\bar{n}_m^T + 1)$ contributes to the derivative of V, and the approximation equation shown by Eq. (25) is not valid. Therefore, Δp^2 will not decrease monotonically with time evolution, which leads to the squeezing level S decreasing with large $\bar{n}_m^T$. Nevertheless, we can get relatively large squeezing over a long period of time when the thermal phonon number $\bar{n}_m^T$ is not very large. For the thermal phonon number larger than 10^3, one should employ other methods to reduce the temperature of the bath before using Lyapunov control.

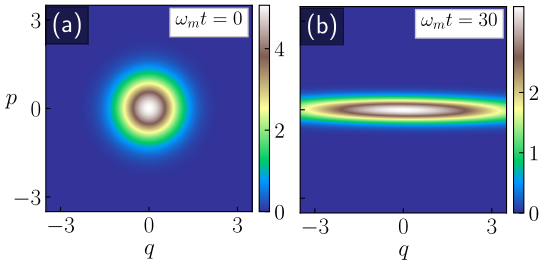

Fig. 4. Wigner function in units of 1/100 for $\omega_m t = 0$ and $\omega_m t = 30$ in (a) and (b), respectively. The parameters are the same as in Fig. 2(a).

5. DETECTION OF MECHANICAL SQUEEZING

Finally, we discuss the detection of the generated mechanical squeezing in our scheme. As depicted in Fig. 1, an ancillary cavity mode a_s with frequency ω_s is introduced to the system for detection. Meanwhile, the ancillary mode a_s is driven by a weak pump field with amplitude E_p and frequency ω_p. The total Hamiltonian with the ancillary mode included is

$$H_t = H + \hbar\omega_s a_s^\dagger a_s - \hbar g_s a_s^\dagger a_s q + i\hbar E_p(e^{-i\omega_p t}a_s^\dagger - \text{h.c.}), \tag{28}$$

where H is given by Eq. (7), and g_s is the coupling strength between the ancillary mode a_s and the mechanical oscillator. The pump field of a_s is selected to be very weak so that the ancillary mode reaches a small steady-state amplitude α_s, i.e., $\alpha_s \ll \alpha$, thus $G_s \ll G$. Therefore, we can safely neglect the backaction of a_s on the mechanical oscillator, and the dynamics of mechanical mode δq (δp) and cavity mode δX (δY) can still be well described by Eq. (12). We will discuss the correction later. Now we describe the detection of the squeezing. With the dissipation κ_s and noise $a_{s,\text{in}}$ taken into consideration, the linearized equation for the ancillary mode a_s is

$$\dot{\delta a}_s = -(\kappa_s + i\Delta_s')\delta a_s + iG_s\delta q + \sqrt{2\kappa_s}a_{s,\mathrm{in}}, \tag{29}$$

where Δ_s' is the effective detuning. If we choose parameters so that $\Delta_s' = \omega_m \gg G_s/\sqrt{2}$, κ_s, by neglecting the terms rapidly oscillating at the frequency $2\omega_m$, the above equation can be rewritten as

$$\dot{\delta a}_s = -(\kappa_s + i\Delta_s')\delta a_s + i\frac{G_s}{\sqrt{2}}\delta b + \sqrt{2\kappa_s}a_{s,\mathrm{in}}, \tag{30}$$

where $\delta b = (i\delta p + \delta q)/\sqrt{2}$. Under $\kappa_s \gg G_s/\sqrt{2}$, the ancillary mode δa_s will adiabatically follow the dynamics of δb [57], and is given by

$$\delta a_s = \frac{iG_s}{\sqrt{2}(\kappa_s + i\Delta_s')}\delta b + \frac{\sqrt{2\kappa_s}}{\kappa_s + i\Delta_s'}a_{s,\mathrm{in}}. \tag{31}$$

Using the input–output relation $\delta a_{s,\mathrm{out}} = \sqrt{2\kappa_s}\delta a_s - \delta a_{s,\mathrm{in}}$, we have

$$\delta a_{s,\mathrm{out}} = \frac{i\sqrt{\kappa_s}G_s}{\kappa_s + i\Delta_s'}\delta b + \left(\frac{2\kappa_s}{\kappa_s + i\Delta_s'} - 1\right)a_{s,\mathrm{in}}. \tag{32}$$

The above equation shows that the output field of the ancillary mode gives a direct measurement of the mechanical oscillator. This method has been proposed to detect the entanglement between the cavity field and mechanical oscillator [58]. Here we use it to measure the momentum variance of the mechanical oscillator. By defining the quadrature operator $\delta X_{s,\mathrm{out}}(\phi) = (\delta a_{s,\mathrm{out}}e^{-i\phi} + \delta a_{s,\mathrm{out}}^{\dagger}e^{i\phi})/\sqrt{2}$, one can obtain

$$\delta X_{s,\mathrm{out}}(\phi) = \frac{G_s\sqrt{\kappa_s}(\Delta_s'\cos\phi + \kappa_s\sin\phi)}{\Delta_s'^2 + \kappa_s^2}\delta q + \frac{G_s\sqrt{\kappa_s}(\Delta_s'\sin\phi - \kappa_s\cos\phi)}{\Delta_s'^2 + \kappa_s^2}\delta p + F_{ad}, \tag{33}$$

where F_{ad} is the noise term. By choosing appropriate ϕ such that $\tan\phi = -\Delta_s'/\kappa_s$, the term that contains δq is removed, and we can obtain

$$\delta X_{s,\mathrm{out}}(\phi) = \frac{G_s\sqrt{\kappa_s}(\Delta_s'\sin\phi - \kappa_s\cos\phi)}{\Delta_s'^2 + \kappa_s^2}\delta p + F_{ad}. \tag{34}$$

It is obvious that δp can be directly reflected in $\delta X_{s,\mathrm{out}}(\phi)$. Therefore, we can detect the generated squeezing of the mechanical mode by measuring the variance of the output ancillary mode $\delta X_{s,\mathrm{out}}(\phi)$. However, it should be recognized from Eq. (34) that $\delta X_{s,\mathrm{out}}(\phi)$ is a weak signal. In order to amplify the signal, the balanced homodyne detection method is used here, where the local oscillator (LO) noise is simultaneously eliminated. As illustrated in Fig. 1, the signal field $\delta a_{s,\mathrm{out}}$ first passes through a phase shifter to rotate a phase $\pi/2 + \phi$, where $\pi/2$ is used to compensate for the phase shift between the reflected and incident field in the polarizing beam splitter (PBS), and ϕ is used to rotate the field $\delta a_{s,\mathrm{out}}$ by a phase ϕ so as to detect the momentum variance of the mechanical oscillator. Then the rotated field $\delta a_{s,\mathrm{out}}$ is superimposed with a strong LO through a 50/50 beam splitter, in which the output signal is

$$n_{cd} = -i(|\beta_l|e^{-i\phi_l}\delta a_{s,\mathrm{out}}^{\dagger} - |\beta_l|e^{i\phi_l}\delta a_{s,\mathrm{out}}), \tag{35}$$

where $|\beta_l|$ and ϕ_l are respectively the amplitude and phase of LO. Therefore, the variance of the output signal is

$$(\Delta n_{cd})^2 = 4|\beta_l|^2\Delta X_{s,\mathrm{out}}^2(\phi_l + \pi/2), \tag{36}$$

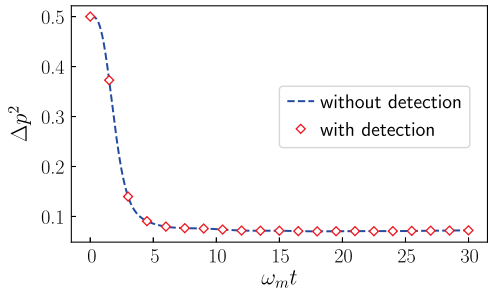

Fig. 6. Time evolution of Δq^2 with detection and without detection, where $G_s/\omega_m = 0.01$ and $\kappa_s/\omega_m = 0.1$. The other parameters are the same as in Fig. 2(a).

where $\Delta X_{s,\mathrm{out}}^2(\phi) = \langle\delta X_{s,\mathrm{out}}^2(\phi)\rangle - \langle\delta X_{s,\mathrm{out}}(\phi)\rangle^2$. From the above equation, we see that the weak signal $\Delta X_{s,\mathrm{out}}^2(\phi_l + \pi/2)$ is amplified in the detection by an amplification factor $4|\beta_l|^2$. By substituting Eq. (34) into Eq. (36), and setting the phase of the LO $\phi_l = \pi/2 - \phi$, we can get the relationship between the oscillator variance Δp^2 and $(\Delta n_{cd})^2$; therefore, the generated mechanical squeezing can be detected by the proposal discussed above.

It should be noted that the backaction of a_s on the mechanical oscillator is neglected in the detection proposal. Whether the added ancillary mode a_s can affect the dynamics of the mechanical oscillator or not should be verified. Therefore, it is necessary to compare the dynamics of the mechanical oscillator with and without the ancillary mode. By taking the system with the ancillary detection mode a_s into consideration, the dynamics equation of the 6×6 covariance matrix R' satisfies

$$\dot{R}'(t) = A'(t)R'(t) + R'(t)A'^{T}(t) + D', \tag{37}$$

where $D' = \mathrm{Diag}[\kappa, \kappa, 0, \gamma(2\bar{n}_m^T + 1), \kappa_s, \kappa_s]$, and

$$A'(t) = \begin{pmatrix} -k & \Delta_c' & 0 & 0 & 0 & 0 \\ -\Delta_c' & -\kappa & \sqrt{2}G & 0 & 0 & 0 \\ 0 & 0 & 0 & \omega_m & 0 & 0 \\ \sqrt{2}G & 0 & -\frac{\omega_r^2(t)}{\omega_m} & -\gamma & \sqrt{2}G_s & 0 \\ 0 & 0 & 0 & 0 & -\kappa_s & \Delta_s' \\ 0 & 0 & \sqrt{2}G_s & 0 & -\Delta_s' & -\kappa_s \end{pmatrix}. \tag{38}$$

To examine the influence on the system of the ancillary detection mode, we present the time evolution of Δq^2 with and without the detection mode together in Fig. 6, where the control field designed in Fig. 2(c) is used for both of the two cases. The result shows that the evolution of Δq^2 agrees very well for the two cases. Therefore, we can safely neglect the backaction of a_s on the mechanical oscillator.

6. DISCUSSION AND CONCLUSIONS

We now discuss the experimental feasibility of our scheme. For the cavity optomechanical system, $\kappa/\omega_m = 10^{-2}$–$10$ and $\gamma/\omega_m = 10^{-9}$–$10$ have been reported in experiments (see Table II in Ref. [59]). Obviously the parameters $\kappa/\omega_m = 0.1$, $\gamma/\omega_m = 10^{-6}$ used in our simulations are within the current

experiments. From Fig. 2, we know that the squeezing process is fast, and hence we can assume that $\bar{n}_m^T$ is not affected by the tuning frequency $\nu(t)$ but only determined by the static frequency ω_m; therefore, the thermal phonon number is evaluated by $\bar{n}_m^T = [\exp(\hbar\omega_m/k_B T) - 1]^{-1}$. Moreover, if the frequency of the mechanical oscillator is tuned by the method described in Appendix A, the thermal phonon number of the mechanical oscillator $\bar{n}_m$ is just determined by the frequency of the mechanical oscillator ω_m after ignoring the vacuum noise from the ancillary cavity. In Fig. 5(b), the thermal phonon numbers $\bar{n}_m^T = 10, 10^3$, and 10^4 are corresponding to the temperature of the bath $T = 0.01$ K, 0.9 K, and 9.6 K, respectively, when frequency of the mechanical oscillator is $\omega_m/2\pi = 20$ MHz. Currently, the temperature of thermal bath $T = 10$ mK has been reported experimentally, and thus the proposed scheme is achievable within the current experiments.

In addition, the frequency-tunable mechanical oscillator has been realized experimentally [52–54], and we also give an alternative method to tune the mechanical frequency in Appendix A, which is experimentally feasible. For many proposals realizing mechanical squeezing, the squeezing level is limited by the 3 dB limit due to the unsteadiness of the system caused by the parametric amplification process. However, in our scheme, the frequency of the mechanical oscillator is time-dependent and is designed by the Lyapunov control method, which can guarantee that the fluctuation of the mechanical mode always decreases with time evolution without divergence [see the evolution of Δq^2 in Figs. 2(a) and 2(b)]. Therefore, the system can be stable with the squeezing level beyond 3 dB.

To conclude, in this paper, by using the Lyapunov control method, we have presented a scheme for generating mechanical squeezing. By designing the time-varying mechanical frequency, the momentum variance of the mechanical mode can decrease with the time evolution under the weak coupling case. As a consequence, the squeezing exceeding the 3 dB limit is obtained quickly, and the largest squeezing can be larger than 10 dB. In addition, the squeezing is robust against cavity decay for the weak coupling regime. In the strong coupling case, the obtained squeezing is not as good as the weak coupling case due to the backaction. Although the mechanical thermal phonon number can destroy the preparation of mechanical squeezing, we can obtain strong squeezing at the temperature within the current experiment technology. In addition, we discuss the detection of the momentum variance Δp^2 by introducing an ancillary mode. Via homodyne detection, we simulate Δp^2 with and without an ancillary mode. The results show that the backaction of the ancillary mode can be ignored, which ensures the validity of the detection protocol. Our scheme provides a potential way for realizing squeezing of the mechanical motion beyond 3 dB.

APPENDIX A: AN ALTERNATIVE METHOD OF REALIZING TIME-DEPENDENT MECHANICAL FREQUENCY

In this appendix, by using a low-Q mode, we give an alternative method to realize the time-dependent mechanical frequency. The linearized Hamiltonian with the low-Q mode d coupled to the system reads

$$H = \hbar\Delta_c'\delta a^\dagger\delta a + \hbar\Delta_d'\delta d^\dagger\delta d + \frac{\omega_m}{2}(\delta p^2 + \delta q^2) - G(\delta a + \delta a^\dagger)\delta q - G_d(\delta d + \delta d^\dagger)\delta q, \quad \textbf{(A1)}$$

where Δ_d' is the effective detuning between the mode δd and its driving. G_d is the effective coupling between the mode δd and the mechanical oscillator. Different from the case discussed in Section 5 that weak effective coupling G_s is needed, here G_d should not be weak. The Langevin equations are

$$\begin{aligned}\dot{\delta q} &= \omega_m\delta p,\\ \dot{\delta p} &= -\omega_m\delta q - \gamma\delta p + G(\delta a^\dagger + \delta a) + G_d(\delta d^\dagger + \delta d) + \xi,\\ \dot{\delta d} &= -(\kappa_d + i\Delta_d)\delta d + iG_d\delta q + \sqrt{2\kappa}d_{\text{in}}.\end{aligned} \quad \textbf{(A2)}$$

At low-Q condition of mode d, i.e., $\kappa_d \gg \omega_m$, we can eliminate the mode δd by an adiabatical method [60]. Then the equations for δq and δp become

$$\begin{aligned}\dot{\delta q} &= \omega_m\delta p,\\ \dot{\delta p} &= -\left(\omega_m - \frac{2G_d^2\Delta_d}{\Delta_d^2 + \kappa_d^2}\right)\delta q - \gamma\delta p + G(\delta a^\dagger + \delta a) + \xi'.\end{aligned} \quad \textbf{(A3)}$$

Therefore, the effective Hamiltonian after eliminating the low-Q mode d is

$$H = \hbar\Delta\delta' a^\dagger\delta a + \frac{\hbar\omega_m}{2}\delta p^2 + \frac{\hbar\omega_r^2(t)}{2\omega_m}\delta q^2 - \hbar G(\delta a^\dagger + \delta a)\delta q, \quad \textbf{(A4)}$$

where $\omega_r^2(t)/\omega_m = \omega_m - \frac{2G_d^2\Delta_d}{\Delta_d^2+\kappa_d^2}$ has been set. Therefore, we can modulate Δ_d with time evolution to realize the time-dependent mechanical frequency $\omega_r(t)$. In this method, ξ' contains the noise from mode δd as shown in Eq. (A3), and thus it may be not as good as the method by applying a voltage between the mechanical oscillator and the underlying electrode. Hence in the main text, we employ the latter one as an example to illustrate the proposal. Nevertheless, this is an alternative method of realizing time-dependent mechanical frequency. And effective Hamiltonian described by Eq. (A4) can also give the same quantum Langevin equations used in Eq. (11).

Funding. National Natural Science Foundation of China (11874099, 11704026, 11474044); China Postdoctoral Science Foundation funded project (2018T110039).

Acknowledgment. We would like to thank Mr. Ye-Xiong Zeng, Cheng-Hua Bai and Ming-Hui Du for helpful discussions. Many thanks to Prof. Ying Gu for constructive suggestions.

REFERENCES

1. E. E. Wollman, C. U. Lei, A. J. Weinstein, J. Suh, A. Kronwald, F. Marquardt, A. A. Clerk, and K. C. Schwab, "Quantum squeezing of motion in a mechanical resonator," Science **349**, 952–955 (2015).
2. C.-S. Hu, Z.-B. Yang, H. Wu, Y. Li, and S.-B. Zheng, "Twofold mechanical squeezing in a cavity optomechanical system," Phys. Rev. A **98**, 023807 (2018).
3. W. H. Zurek, "Decoherence and the transition from quantum to classical," Phys. Today **44**, 36–44 (1991).

4. S.-L. Ma, X.-K. Li, J.-K. Xie, and F.-L. Li, "Two-mode squeezed states of two separated nitrogen-vacancy-center ensembles coupled via dissipative photons of superconducting resonators," Phys. Rev. A **99**, 012325 (2019).
5. V. Peano, H. G. L. Schwefel, C. Marquardt, and F. Marquardt, "Intracavity squeezing can enhance quantum-limited optomechanical position detection through deamplification," Phys. Rev. Lett. **115**, 243603 (2015).
6. B. Xie and S. Feng, "Squeezing-enhanced heterodyne detection of 10 Hz atto-Watt optical signals," Opt. Lett. **43**, 6073–6076 (2018).
7. A. Motazedifard, F. Bemani, M. H. Naderi, R. Roknizadeh, and D. Vitali, "Force sensing based on coherent quantum noise cancellation in a hybrid optomechanical cavity with squeezed-vacuum injection," New J. Phys. **18**, 073040 (2016).
8. J. Aasi, J. Abadie, B. P. Abbott, R. Abbott, T. D. Abbott, M. R. Abernathy, C. Adams, T. Adams, P. Addesso, and R. X. Adhikari, "Enhanced sensitivity of the LIGO gravitational wave detector by using squeezed states of light," Nat. Photonics **7**, 613–619 (2013).
9. M. A. Lemonde, N. Didier, and A. A. Clerk, "Enhanced nonlinear interactions in quantum optomechanics via mechanical amplification," Nat. Commun. **7**, 11338 (2016).
10. Y. Wang, C. Li, E. M. Sampuli, J. Song, Y. Jiang, and Y. Xia, "Enhancement of coherent dipole coupling between two atoms via squeezing a cavity mode," Phys. Rev. A **99**, 023833 (2019).
11. X.-Y. Lü, Y. Wu, J. R. Johansson, H. Jing, J. Zhang, and F. Nori, "Squeezed optomechanics with phase-matched amplification and dissipation," Phys. Rev. Lett. **114**, 093602 (2015).
12. D. Rugar and P. Grütter, "Mechanical parametric amplification and thermomechanical noise squeezing," Phys. Rev. Lett. **67**, 699–702 (1991).
13. W. Ge and M. Bhattacharya, "Single and two-mode mechanical squeezing of an optically levitated nanodiamond via dressed-state coherence," New J. Phys. **18**, 103002 (2016).
14. A. Serafini, A. Retzker, and M. B. Plenio, "Generation of continuous variable squeezing and entanglement of trapped ions in time-varying potentials," Quantum Inform. Process. **8**, 619 (2009).
15. W.-Z. Zhang, Y. Han, B. Xiong, and L. Zhou, "Optomechanical force sensor in a non-Markovian regime," New J. Phys. **19**, 083022 (2017).
16. J. Liu and K.-D. Zhu, "Coupled quantum molecular cavity optomechanics with surface plasmon enhancement," Photon. Res. **5**, 450–456 (2017).
17. B. Xiong, X. Li, X.-Y. Wang, and L. Zhou, "Improve microwave quantum illumination via optical parametric amplifier," Ann. Phys. **385**, 757–768 (2017).
18. J. Liu and K.-D. Zhu, "Room temperature optical mass sensor with an artificial molecular structure based on surface plasmon optomechanics," Photon. Res. **6**, 867–874 (2018).
19. A. Motazedifard, A. Dalafi, M. Naderi, and R. Roknizadeh, "Strong quadrature squeezing and quantum amplification in a coupled Bose-Einstein condensate-optomechanical cavity based on parametric modulation," Ann. Phys. **405**, 202–219 (2019).
20. B. A. Levitan, A. Metelmann, and A. A. Clerk, "Optomechanics with two-phonon driving," New J. Phys. **18**, 093014 (2016).
21. X. Xu and J. M. Taylor, "Squeezing in a coupled two-mode optomechanical system for force sensing below the standard quantum limit," Phys. Rev. A **90**, 043848 (2014).
22. J.-Q. Liao and C. K. Law, "Parametric generation of quadrature squeezing of mirrors in cavity optomechanics," Phys. Rev. A **83**, 033820 (2011).
23. C.-H. Bai, D.-Y. Wang, S. Zhang, and H.-F. Wang, "Qubit-assisted squeezing of mirror motion in a dissipative cavity optomechanical system," Sci. China Phys. Mech. Astron. **62**, 970311 (2019).
24. B. Xiong, X. Li, S.-L. Chao, and L. Zhou, "Optomechanical quadrature squeezing in the non-Markovian regime," Opt. Lett. **43**, 6053–6056 (2018).
25. Z.-C. Zhang, Y.-P. Wang, Y.-F. Yu, and Z.-M. Zhang, "Quantum squeezing in a modulated optomechanical system," Opt. Express **26**, 11915–11927 (2018).
26. M. Rashid, T. Tufarelli, J. Bateman, J. Vovrosh, D. Hempston, M. S. Kim, and H. Ulbricht, "Experimental realization of a thermal squeezed state of levitated optomechanics," Phys. Rev. Lett. **117**, 273601 (2016).
27. D. Y. Wang, C. H. Bai, H. F. Wang, A. D. Zhu, and S. Zhang, "Steady-state mechanical squeezing in a double-cavity optomechanical system," Sci. Rep. **6**, 38559 (2016).
28. G. Milburn and D. Walls, "Production of squeezed states in a degenerate parametric amplifier," Opt. Commun. **39**, 401–404 (1981).
29. M. O. Scully and M. S. Zubairy, *Quantum Optics* (Cambridge University, 1997).
30. G. S. Agarwal and S. Huang, "Strong mechanical squeezing and its detection," Phys. Rev. A **93**, 043844 (2016).
31. K. Jähne, C. Genes, K. Hammerer, M. Wallquist, E. S. Polzik, and P. Zoller, "Cavity-assisted squeezing of a mechanical oscillator," Phys. Rev. A **79**, 063819 (2009).
32. A. Dalafi, M. H. Naderi, and A. Motazedifard, "Effects of quadratic coupling and squeezed vacuum injection in an optomechanical cavity assisted with a Bose-Einstein condensate," Phys. Rev. A **97**, 043619 (2018).
33. M. Asjad, G. S. Agarwal, M. S. Kim, P. Tombesi, G. D. Giuseppe, and D. Vitali, "Robust stationary mechanical squeezing in a kicked quadratic optomechanical system," Phys. Rev. A **89**, 023849 (2014).
34. C.-H. Bai, D.-Y. Wang, S. Zhang, S. Liu, and H.-F. Wang, "Engineering of strong mechanical squeezing via the joint effect between duffing nonlinearity and parametric pump driving," Photon. Res. **7**, 1229–1239 (2019).
35. A. Szorkovszky, A. C. Doherty, G. I. Harris, and W. P. Bowen, "Mechanical squeezing via parametric amplification and weak measurement," Phys. Rev. Lett. **107**, 213603 (2011).
36. A. Kronwald, F. Marquardt, and A. A. Clerk, "Arbitrarily large steady-state bosonic squeezing via dissipation," Phys. Rev. A **88**, 063833 (2013).
37. C. U. Lei, A. J. Weinstein, J. Suh, E. E. Wollman, A. Kronwald, F. Marquardt, A. A. Clerk, and K. C. Schwab, "Quantum nondemolition measurement of a quantum squeezed state beyond the 3 dB limit," Phys. Rev. Lett. **117**, 100801 (2016).
38. X. You, Z. Li, and Y. Li, "Strong quantum squeezing of mechanical resonator via parametric amplification and coherent feedback," Phys. Rev. A **96**, 063811 (2017).
39. R. Zhang, Y. Fang, Y.-Y. Wang, S. Chesi, and Y.-D. Wang, "Strong mechanical squeezing in an unresolved-sideband optomechanical system," Phys. Rev. A **99**, 043805 (2019).
40. J.-M. Pirkkalainen, E. Damskägg, M. Brandt, F. Massel, and M. A. Sillanpää, "Squeezing of quantum noise of motion in a micromechanical resonator," Phys. Rev. Lett. **115**, 243601 (2015).
41. W.-J. Gu, Z. Yi, L.-H. Sun, and Y. Yan, "Generation of mechanical squeezing and entanglement via mechanical modulations," Opt. Express **26**, 30773–30785 (2018).
42. C. Li, J. Song, Y. Xia, and W. Ding, "Driving many distant atoms into high-fidelity steady state entanglement via Lyapunov control," Opt. Express **26**, 951–962 (2018).
43. S. Kuang and S. Cong, "Lyapunov control methods of closed quantum systems," Automatica **44**, 98–108 (2008).
44. D. Ran, W.-J. Shan, Z.-C. Shi, Z.-B. Yang, J. Song, and Y. Xia, "High fidelity Dicke-state generation with Lyapunov control in circuit QED system," Ann. Phys. **396**, 44–55 (2018).
45. W. Li, C. Li, and H. Song, "Quantum synchronization in an optomechanical system based on Lyapunov control," Phys. Rev. E **93**, 062221 (2016).
46. D. Ran, Z.-C. Shi, J. Song, and Y. Xia, "Speeding up adiabatic passage by adding Lyapunov control," Phys. Rev. A **96**, 033803 (2017).
47. Z. C. Shi, L. C. Wang, and X. X. Yi, "Preparing entangled states by Lyapunov control," Quantum Inform. Process. **15**, 4939–4953 (2016).
48. Y.-X. Zeng, T. Gebremariam, M.-S. Ding, and C. Li, "Quantum optical diode based on Lyapunov control in a superconducting system," J. Opt. Soc. Am. B **35**, 2334–2341 (2018).
49. W.-M. Zhang, K.-M. Hu, Z.-K. Peng, and G. Meng, "Tunable micro- and nanomechanical resonators," Sensors **15**, 26478–26566 (2015).
50. D.-Y. Wang, C.-H. Bai, S. Liu, S. Zhang, and H.-F. Wang, "Optomechanical cooling beyond the quantum backaction limit with frequency modulation," Phys. Rev. A **98**, 023816 (2018).
51. A. Farace and V. Giovannetti, "Enhancing quantum effects via periodic modulations in optomechanical systems," Phys. Rev. A **86**, 013820 (2012).

52. R. A. Barton, I. R. Storch, V. P. Adiga, R. Sakakibara, B. R. Cipriany, B. Ilic, S. P. Wang, P. Ong, P. L. McEuen, J. M. Parpia, and H. G. Craighead, "Photothermal self-oscillation and laser cooling of graphene optomechanical systems," Nano Lett. **12**, 4681–4686 (2012).
53. C. Chen, S. Lee, V. V. Deshpande, G.-H. Lee, M. Lekas, K. Shepard, and J. Hone, "Graphene mechanical oscillators with tunable frequency," Nat. Nanotechnol. **8**, 923–927 (2013).
54. V. Singh, S. Bosman, B. Schneider, Y. M. Blanter, A. Castellanos-Gomez, and G. Steele, "Optomechanical coupling between a multilayer graphene mechanical resonator and a superconducting microwave cavity," Nat. Nanotechnol. **9**, 820–824 (2014).
55. J.-Q. Liao and C. K. Law, "Cooling of a mirror in cavity optomechanics with a chirped pulse," Phys. Rev. A **84**, 053838 (2011).
56. Y.-D. Wang and A. A. Clerk, "Using interference for high fidelity quantum state transfer in optomechanics," Phys. Rev. Lett. **108**, 153603 (2012).
57. X.-Y. Lü, J.-Q. Liao, L. Tian, and F. Nori, "Steady-state mechanical squeezing in an optomechanical system via duffing nonlinearity," Phys. Rev. A **91**, 013834 (2015).
58. D. Vitali, S. Gigan, A. Ferreira, H. R. Böhm, P. Tombesi, A. Guerreiro, V. Vedral, A. Zeilinger, and M. Aspelmeyer, "Optomechanical entanglement between a movable mirror and a cavity field," Phys. Rev. Lett. **98**, 030405 (2007).
59. M. Aspelmeyer, T. J. Kippenberg, and F. Marquardt, "Cavity optomechanics," Rev. Mod. Phys. **86**, 1391–1452 (2014).
60. Y.-C. Liu, Y.-F. Xiao, X. Luan, Q. Gong, and C. W. Wong, "Coupled cavities for motional ground-state cooling and strong optomechanical coupling," Phys. Rev. A **91**, 033818 (2015).